Electrochimica Acta xxx (2012) xxx–xxx

Contents lists available at SciVerse ScienceDirect

Electrochimica Acta

journal homepage: www.elsevier.com/locate/electacta

# Gold nanoparticles-coated poly(3,4-ethylene-dioxythiophene) for the selective determination of sub-nano concentrations of dopamine in presence of sodium dodecyl sulfate

Nada F. Atta*, Ahmed Galal, Ekram H. El-Ads

*Department of Chemistry, Faculty of Science, Cairo University, 12613 Giza, Egypt*

ARTICLE INFO

*Article history:*
Received 26 November 2011
Received in revised form 21 February 2012
Accepted 22 February 2012
Available online xxx

*Keywords:*
Sensor
PEDOT
Gold nanoparticles
SDS
Dopamine
Ascorbic acid

ABSTRACT

For the first time, a novel electrochemical sensor; gold nanoparticles-coated poly(3,4-ethylene-dioxythiophene) polymer modified gold electrode in presence of SDS (Au/PEDOT-$Au_{nano}$...SDS) was developed by the electrodeposition of gold nanoparticles on poly(3,4-ethylene-dioxythiophene) (PEDOT) modified gold electrode for the selective determination of dopamine (DA) in presence of uric acid (UA) and ascorbic acid (AA) in presence of sodium dodecyl sulfate (SDS). Synergism between the composite of conducting polymer matrix and gold nanoparticles in presence of SDS for electron transfer enhancement of DA is explored. Electrochemical investigation and characterization of the modified electrode are achieved using cyclic voltammetry, electrochemical impedance spectroscopy, scanning electron, and atomic force microscopies. The oxidation current signal of DA is remarkably stable via repeated cycles and has unique long term stability. Very small peak potential separation ($\Delta E_p$), almost zero or 15 mV is also obtained by repeated cycles indicating unusual high reversibility. The use of SDS in the electrochemical determination of DA using linear sweep voltammetry at Au/PEDOT-$Au_{nano}$ modified electrode resulted in determining DA at very low concentrations. The DA concentration could be measured in the linear range of 0.5–20 $\mu mol\,L^{-1}$ and 25–140 $\mu mol\,L^{-1}$ with correlation coefficients of 0.9978, and 0.9987, and detection limits of 0.39 $nmol\,L^{-1}$ and 1.55 $nmol\,L^{-1}$, respectively. The validity of using this method in the determination of DA in human urine was also demonstrated. It has been shown that modified electrode can be used as a sensor with high reproducibility, sensitivity, selectivity, and long term stability.


## 1. Introduction

Recent activities in electroanalytical chemistry have focused on the development of nano-scaled particles in sensor and biosensor applications, due to its unique physicochemical, optical, magnetic, and electronic characteristics that are significantly different from those of bulk materials [1–8]. Particularly, gold nanoparticles ($Au_{nano}$) have potential applications in the construction of electrochemical sensors and biosensors due to their advantages of enhanced diffusion [1,9], good stability and biocompatibility in biomolecules detection [2,5,9], high effective surface area, improved selectivity and sensitivity, outstanding electrocatalytic activity, good conductivity, and high signal-to-noise ratio [1,2,4,10,11]. They function as "electron antennae" efficiently channeling electrons between the electrode and the electroactive species promoting better electron transfer between the electrode surface and the electrolyte [4]. Gold nanoparticles dispersed on a variety of substrates have been reported in literature, such as indium tin oxide [3,4,6,10], highly ordered pyrolytic graphite (HOPG) [1], choline [1], carbon nanotubes [9], carbon paste electrode [11], self-assembled monolayer [5], and polymers [7,8,12]. Concerning electrochemically generated polymers, attention has been devoted since the mid-1990s to poly(3,4-ethylenedioxythiophene) (PEDOT). This polymer induces uniform and adherent polymer film on most of electrode materials, shows quite high conductivity in its oxidized state and a low band-gap, presents good stability in aqueous electrolytes and has biocompatibility with biological media [13–18]. Conducting polymer incorporated metallic or semiconducting nanoparticles provides an exciting system and these materials hold potential application in electronics, sensors, biosensors and catalysis. They have synergistic chemical and physical properties based on the constituent polymer and introduced metal [19–23]. By tuning the polymer backbone with nanoscale materials, realization of nano-electronic sensor devices with superior performance is possible [23]. Gold nanoparticles can be grown inside the PEDOT matrix by chemical routes [24–27] or by simultaneous electrodeposition of polymer along with metal nanoparticles [23,28–31] or by electrochemical

* Corresponding author. Tel.: +20 0237825266; fax: +20 0235727556.
*E-mail address:* nada_fah1@yahoo.com (N.F. Atta).

0013-4686/$ – see front matter © 2012 Elsevier Ltd. All rights reserved.
doi:10.1016/j.electacta.2012.02.082

deposition of gold nanoparticles on the PEDOT prepared by spin coating method [32] or on the electropolymerized PEDOT [33]. DA is one of the important neurotransmitters that are widely distributed in the mammalian central nervous system for message transfer [11,34]. It plays a very important role in the functioning of central nervous, renal, hormonal, and cardiovascular systems. Thus, a loss of DA-containing neurons may lead to neurological disorders such as Parkinsonism and schizophrenia [11,17,19–22]. Simultaneous detection of DA, ascorbic acid (AA) and uric acid (UA) is a problem of critical importance not only in the field of biomedical chemistry and neurochemistry but also for diagnostic and pathological research [34–36]. At bare electrodes, the selective determination of AA, DA, and UA is impossible because their oxidation potentials are very close. Besides, stability and reproducibility cannot be achieved at bare electrodes due to the surface fouling caused by the adsorption of oxidized products of AA on electrode surface [11,17]. To overcome these problems, various modified electrodes have been constructed such as polymer films [17,37], polymer–metal nanoparticles composites [7,19–22,38], self-assembled monolayers [5,39,40], and gold nanoparticles [4,11,34,41] modified electrodes. PEDOT incorporated gold nanoparticles have been used to simultaneously determine DA, AA, and UA [28,30]. Surfactants, a kind of amphiphilic molecules with a hydrophilic head on one side and a long hydrophobic tail on the other, have been widely applied in electrochemistry to improve the property of the electrode/solution interface [17,41–45]. Surfactants have proven effective in the electroanalysis of biological compounds and drugs [42,43]. Different modified electrodes were used for the selective determination of DA in presence of sodium dodecyl sulfate SDS [17,44,45].

In the current study, a novel modified electrode (Au/PEDOT-$Au_{nano}$) was fabricated by the electrodeposition of gold nanoparticles into the electropolymerized PEDOT film over the surface of gold (Au) electrode. Au/PEDOT-$Au_{nano}$ modified electrode was used for the first time for determination of DA in presence of SDS (Au/PEDOT-$Au_{nano}$...SDS). The voltammetric response of Au/PEDOT-$Au_{nano}$...SDS is highly selective toward DA compared to Au/PEDOT-$Au_{nano}$. The new composite electrode (Au/PEDOT-$Au_{nano}$...SDS) combines the properties of PEDOT to reduce the oxidation potential with the attractive electrocatalytic properties of gold nanoparticles and SDS to promote a fast electron transfer reaction. The application of the proposed sensor for the simultaneous determination of DA, AA, and UA and separation of tertiary mixture of DA, AA, and acetaminophen APAP proved excellent. Different parameters relevant to sensors were considered such as the reproducibility, sensitivity, selectivity, stability of the redox signals, long term stability as well as detection limits.

## 2. Experimental

### 2.1. Chemicals and reagents

All chemicals were used as received without further purification. 3,4-Ethylene dioxy-thiophene (EDOT), tetrabutylammonium hexafluorophosphate (TBAHFP), acetonitrile ([HPLC] grade), dopamine (DA), uric acid (UA), ascorbic acid (AA), acetaminophen (APAP), sodium dodecyl sulfate (SDS) and hydrogen tetrachloroaurate ($HAuCl_4$) were supplied by Aldrich Chem. Co. (Milwaukee, WI, USA). Aqueous solutions were prepared using double distilled water. Phosphate buffer solution 0.1 mol $L^{-1}$ PBS (1 mol $L^{-1}$ $K_2HPO_4$ and 1 mol $L^{-1}$ $KH_2PO_4$) was used as the supporting electrolyte. pH was adjusted using 0.1 mol $L^{-1}$ $H_3PO_4$ and 0.1 mol $L^{-1}$ KOH.

### 2.2. Electrochemical cells and equipments

Electrochemical polymerization and characterization were carried out with a three-electrode/one compartment glass cell. The working electrode was gold disc (diameter: 1 mm). The auxiliary electrode was in the form of 6.0 cm platinum wire. All the potentials in the electrochemical studies were referenced to Ag/AgCl (4 mol $L^{-1}$ KCl saturated with AgCl) electrode. Working electrode was polished using alumina (2 μM)/water slurry until no visible scratches were observed. Prior to immersion in the cell, the electrode surface was thoroughly rinsed with distilled water and dried. All experiments were performed at 25 ± 0.2 °C.

The electrosynthesis of the PEDOT film, gold nanoparticles and their electrochemical characterization were performed using a BAS-100B electrochemical analyzer (Bioanalytical Systems, BAS, West Lafayette, USA). EIS was performed using a Gamry-750 instrument and a lock-in-amplifier that are connected to a personal computer. The data analysis was provided with the instrument and applied non-linear least square fitting with Levenberg–Marquardt algorithm. All impedance experiments were recorded between 0.1 Hz and 100 kHz with an excitation signal of 10 mV amplitude. The measurements were performed under potentiostatic control at different applied potentials which were decided from the cyclic voltammogram recorded for the modified electrode. Quanta FEG 250 instrument was used to obtain the scanning electron micrographs of the different films. The topographs of Au/PEDOT, Au/PEDOT-$Au_{nano}$, and Au/PEDOT-$Au_{nano}$...SDS electrodes were investigated with atomic force microscopy AFM (SPM, Shimadzu, Japan) using the non-contact mode.

### 2.3. Electropolymerization of EDOT

The polymer film was electrochemically formed by applying a constant potential (1400 mV) to the working Au electrode for 30 s (Bulk Electrolysis, BE). The thickness of the film was controlled by the amount of charge consumed during the electro-polymerization (assuming 100% efficiency during the electrochemical conversion). The synthesis solution consisted of 0.01 mol $L^{-1}$ monomer (3,4-EDOT), and 0.01 mol $L^{-1}$ supporting electrolyte (TBAHFP) dissolved in acetonitrile ([HPLC] grade).

### 2.4. Preparation of PEDOT-$Au_{nano}$ composite electrodes

Briefly, a polymer film is prepared and washed with doubly distilled water. This was followed by the electrochemical deposition of gold nanoparticles from a solution containing 6 mmol $L^{-1}$ $HAuCl_4$ prepared in 0.1 mol $L^{-1}$ $KNO_3$ (prepared in doubly distilled water and deaerated by bubbling with nitrogen). The potential applied between the working Au/PEDOT electrode and the reference Ag/AgCl (4 mol $L^{-1}$ KCl saturated with AgCl) electrode is held constant at −400 mV (Bulk Electrolysis, BE) for 400 s [11]. The surface coverage ($\Gamma$) of gold nanoparticles was approximately $4.4 \times 10^{-6}$ mol/cm$^2$ (estimated from the quantity of charge used in the electrodeposition process). This electrode is denoted as Au/PEDOT-$Au_{nano}$. Further modification is done by the successive additions of 10 μL of 0.1 mol $L^{-1}$ SDS (prepared in distilled water) to the DA solution (1 mmol $L^{-1}$ DA/0.1 mol $L^{-1}$ PBS, pH 2.58, and 7.40) from 0 up to 200 μL (increments add $6.7 \times 10^{-5}$ mol $L^{-1}$ SDS of each addition and the total concentration of SDS after 20 additions is $1.3 \times 10^{-3}$ mol $L^{-1}$) and the electrode is denoted as Au/PEDOT-$Au_{nano}$...SDS. After each addition, stirring takes place for 5 min then holds for 1 min before running the experiment.

### 2.5. Analysis of urine

The utilization of the proposed method in real sample analysis was also investigated by direct analysis of DA in human urine samples. DA was dissolved in urine to make a stock solution with 0.5 mmol $L^{-1}$ concentration. Standard additions were carried out

Please cite this article in press as: N.F. Atta, et al., Gold nanoparticles-coated poly(3,4-ethylene-dioxythiophene) for the selective determination of sub-nano concentrations of dopamine in presence of sodium dodecyl sulfate, Electrochim. Acta (2012), doi:10.1016/j.electacta.2012.02.082

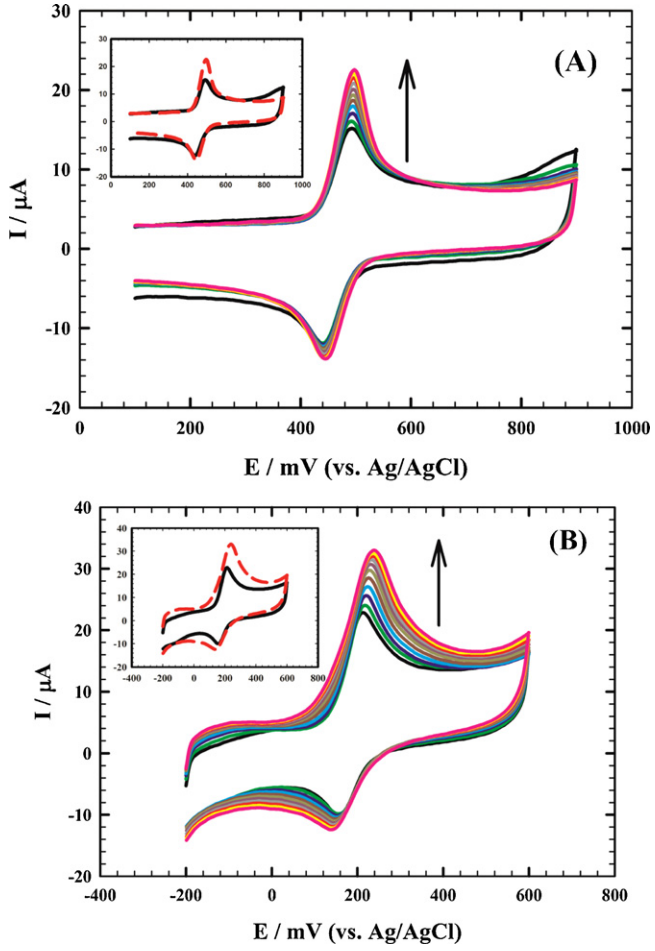


**Fig. 1.** CVs of 1 mmol $L^{-1}$ DA/0.1 mol $L^{-1}$ PBS at Au/PEDOT-$Au_{nano}$ electrode with successive additions (0–200 μl) of 0.1 mol $L^{-1}$ SDS with stirring the solution for 5 min every addition and 1 min for occupation at (A) pH 2.58 and (B) pH 7.40, (increments add $6.7 \times 10^{-5}$ mol $L^{-1}$ SDS of each addition and the total concentration of SDS after 20 additions is $1.3 \times 10^{-3}$ mol $L^{-1}$), inset represents the initial (in absence of SDS) and final (in presence of 200 μL SDS) CVs, scan rate 50 mV $s^{-1}$.

from the DA stock solution in 15 mL of 0.1 mol $L^{-1}$ PBS (pH 7.40) containing 200 μL SDS.

## 3. Results and discussion

### 3.1. Electrochemistry of DA at Au/PEDOT-$Au_{nano}$ in presence of SDS

The voltammetric behavior of DA was examined using cyclic voltammetry. Fig. 1(A) and (B) compares typical cyclic voltammograms of 1 mmol $L^{-1}$ DA in 0.1 mol $L^{-1}$ PBS/pH 2.58 and 7.40 at scan rate 50 mV $s^{-1}$ using PEDOT-$Au_{nano}$ modified Au electrode in presence of 200 μL SDS (Au/PEDOT-$Au_{nano}$...SDS). The inset of Fig. 1(A) and (B) shows the CVs of DA at the modified electrode in the absence and in presence of 200 μL SDS. The successive additions of 10 μL of 0.1 mol $L^{-1}$ SDS (increments add $6.7 \times 10^{-5}$ mol $L^{-1}$ SDS of each addition and the total concentration of SDS after 20 additions is $1.3 \times 10^{-3}$ mol $L^{-1}$) to 1 mmol $L^{-1}$ DA in 0.1 mol $L^{-1}$ PBS/pH 2.58 (Fig. 1(A)) leads to increasing the oxidation and reduction currents of DA from 11.3 μA and 10.1 μA in the absence of SDS to 19.4 μA and 13.2 μA in presence of 200 μL of SDS, respectively. The CV in pH 2.58 is characterized by the appearance of distinct anodic peak at 497 mV and a cathodic peak at 446 mV. The same trend was observed in pH 7.40 (Fig. 1(B)), and the anodic and cathodic peaks of DA appeared at 239 mV and 139 mV, respectively. Also,

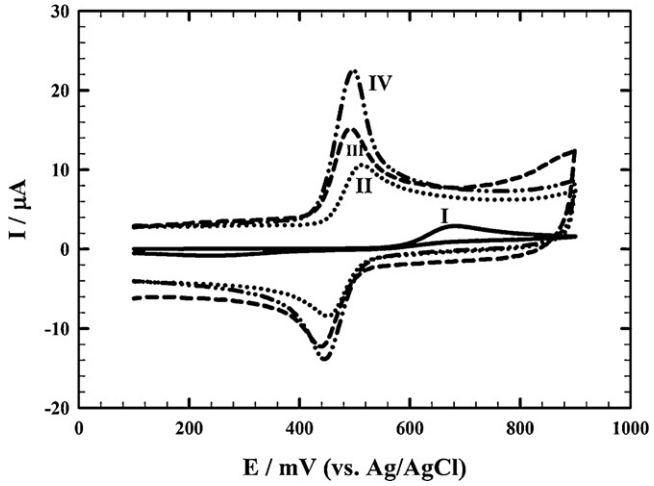


**Fig. 2.** CVs of 1 mmol $L^{-1}$ DA/0.1 mol $L^{-1}$ PBS/pH 2.58 at: (I) bare Au, (II) Au/PEDOT, (III) Au/PEDOT-$Au_{nano}$, and (IV) Au/PEDOT-$Au_{nano}$...SDS modified electrodes, scan rate 50 mV $s^{-1}$.

the oxidation and reduction currents of DA/pH 7.40 increase from 17.6 μA and 10.2 μA in absence of SDS to 28 μA and 13 μA in presence of 200 μL SDS, respectively. The effect of changing the pH of PBS on the voltammetric response of DA was observed. Thus, the oxidation peak potential shifts to a less positive value and the oxidation current response increases as pH increases from 2.58 to 7.40. SDS is an anionic surfactant with hydrophobic tail consisting of 12 carbon atoms and hydrophilic head consisting of sulfate group. The suggested mechanism for the aggregation of surfactants on the modified electrode surface in the form of bilayers, cylinder, or surface micelles (in the case of relatively higher concentrations added of SDS) could explain the increase in the current in the presence of surfactants [17,42,43]. The electron transfer process will take place when the electroactive species approaches the vicinity of the electrode surface. Two main possibilities allow the transfer of charge; first is the displacement of the adsorbed surfactant by the analyte, and second is the approach of the analyte to the surface of the electrode within the space of one to two head groups of adsorbed surfactant moieties. We believe that the second mechanism is more plausible. Furthermore, a possible mechanism suggests the formation of ion-pair that anchor onto the surface of the electrode that should posses some hydrophobic character. Thus, the resulting ion-pair of the charged surfactant and drug tend to adhere to the surface through the lipophilic parts in both moieties [17,42,43]. Thus, the presence of SDS enhances the diffusion of DA through the Au/PEDOT-$Au_{nano}$ modified electrode.

### 3.2. Electrochemistry of DA at different modified electrodes

The oxidation behavior of 1 mmol $L^{-1}$ DA/0.1 mol $L^{-1}$ PBS/pH 2.58 at bare Au, Au/PEDOT, Au/PEDOT-$Au_{nano}$, and Au/PEDOT-$Au_{nano}$...SDS electrodes is shown in Fig. 2. DA undergoes a two-electron oxidation to obtain the o-quinone form (DOQ) of DA [30]. When compared to bare Au electrode, the oxidation current of DA increases by 63%, 75%, and 85% at Au/PEDOT, Au/PEDOT-$Au_{nano}$, and Au/PEDOT-$Au_{nano}$...SDS electrodes, respectively which clearly indicates the catalytic DA oxidation at the modified electrodes. The anodic peak of DA shifted to 513 mV at Au/PEDOT and to about 493 mV at Au/PEDOT-$Au_{nano}$, and Au/PEDOT-$Au_{nano}$...SDS, compared to 683 mV at bare Au electrode. Also, the peak separation ($\Delta E_p$) is found to be 448 mV at bare Au which decreases to 61 mV at Au/PEDOT and to about 51 mV at Au/PEDOT-$Au_{nano}$ and Au/PEDOT-$Au_{nano}$...SDS electrodes. From the previous results, we can conclude that the new composite electrode

Please cite this article in press as: N.F. Atta, et al., Gold nanoparticles-coated poly(3,4-ethylene-dioxythiophene) for the selective determination of sub-nano concentrations of dopamine in presence of sodium dodecyl sulfate, Electrochim. Acta (2012), doi:10.1016/j.electacta.2012.02.082

Au/PEDOT-$Au_{nano}$...SDS combines the properties of PEDOT to reduce the oxidation potential with the attractive electrocatalytic properties of gold nanoparticles and SDS to promote a fast electron transfer reaction. The previous results could be interpreted as follows; the PEDOT film contains a distribution of hydrophobic (reduced) and hydrophilic (oxidized) regions and the hydrophobic $DA^+$ cations prefer to interact with the more hydrophobic regions [23,30]. Also, the PEDOT film has a rich electron cloud that acts as an electron mediator. In addition, a hydrophobic environment appears to favour reversible oxidation of DA. The increase in oxidation current of DA at Au/PEDOT-$Au_{nano}$ is attributed to the favourable weak adsorption of $DA^+$ cations on gold nanoparticles. The weak adsorption of DA on the gold nanoparticles surface may be due to the fact that DA self-assembles on gold surfaces through the interaction of $-NH_2$ group with Au [30] and this clearly indicates the catalytic effect of gold nanoparticles which act as a promoter to enhance the electrochemical reaction, considerably accelerating the rate of electron transfer. The addition of SDS enhances the preconcentration/accumulation of the hydrophobic $DA^+$ cations, accelerates the rate of electron transfer due to the electrostatic attraction of positively charged DA ($pK_a = 8.92$) with the anionic surfactant SDS [17], and enhances the DA current signal at the Au/PEDOT-$Au_{nano}$ modified electrode as discussed before in Section 3.1. PEDOT film reduces the overpotential of DA oxidation when using gold nanoparticles, and SDS improve the sensitivity of DA detection, in other words, Au/PEDOT-$Au_{nano}$...SDS explores the synergism between the PEDOT matrix, gold nanoparticles and SDS for the selective, and sensitive determination of DA. Thus, this modified electrode is used for the first time as a promising electrochemical sensor for DA in presence of AA, and UA.

### 3.3. Effect of scan rate on the voltammetric response of DA

The dependence of the anodic peak current ($I_{pa}$ A) on the scan rate has been used for the estimation of the "apparent" diffusion coefficient $D_{app}$ of 1 mmol $L^{-1}$ DA/0.1 mol $L^{-1}$ PBS/pH 2.58. $D_{app}$ ($cm^2\ s^{-1}$) values were calculated from Randles Sevcik equation (Eq. (1)):

$$I_{pa} = (2.69 \times 10^5)\, n^{3/2} A C_o D^{1/2} \nu^{1/2} \quad (1)$$

where $n$ is the number of electrons exchanged in oxidation at $T = 298$ K, $A$ is the geometrical electrode area = $7.854 \times 10^{-3}$ $cm^2$, $C_o$ is the analyte concentration ($1 \times 10^{-6}$ mol $cm^{-3}$) and $\nu$ is the scan rate V $s^{-1}$ [11,17,19–22]. It is important to notice that the apparent surface area used in the calculations does not take into account the surface roughness, which is inherent characteristic for all polymer films formed using the electrochemical techniques and the surface roughness of gold nanoparticles. The roughness factor calculated from atomic force microscopy measurements of gold nanoparticles in case of Au/PEDOT-$Au_{nano}$ and Au/PEDOT-$Au_{nano}$...SDS are 1.91, and 1.92, respectively and the surface roughness of PEDOT film is 1.52.

Fig. 3 shows the CVs of 1 mmol $L^{-1}$ DA/0.1 mol $L^{-1}$ PBS/pH 2.58 at Au/PEDOT-$Au_{nano}$...SDS at different scan rates (from 10 mV $s^{-1}$ up to 150 mV $s^{-1}$). It can be noticed that a pair of roughly symmetric anodic and cathodic peaks appeared with almost equal peak currents. Moreover, the anodic and cathodic peak currents and the peak-to-peak separation increased with increasing the scan rate [11]. For a diffusion-controlled process, a plot of the anodic peak current values versus the square root of the scan rate results in a straight-line relationship and the inset of Fig. 3 shows a comparison of these linear relationships for DA at Au/PEDOT-$Au_{nano}$ (black circle) and Au/PEDOT-$Au_{nano}$...SDS (white circle) modified electrodes. The oxidation and reduction peak currents increased linearly with the linear regression equations (Eqs. (2) and (3)), respectively at Au/PEDOT-$Au_{nano}$, and (Eqs. (4) and (5)), respectively at Au/PEDOT-$Au_{nano}$...SDS, suggesting that the reaction is diffusion-controlled electrode reaction. $D_{app}$ value is $5.25 \times 10^{-4}$ $cm^2\ s^{-1}$ in presence of SDS and $8.18 \times 10^{-5}$ $cm^2\ s^{-1}$ in absence of SDS.

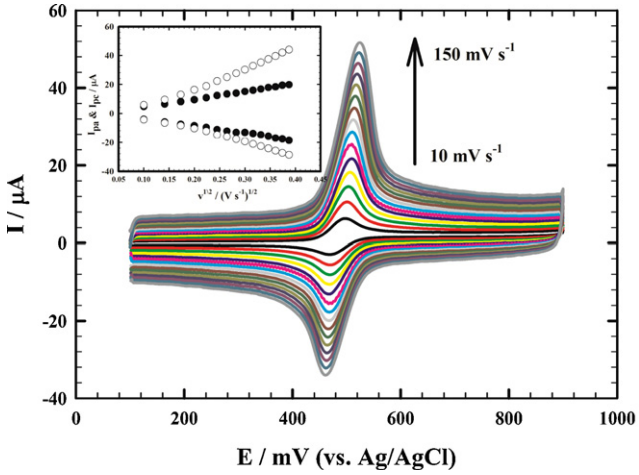


**Fig. 3.** CVs of 1 mmol $L^{-1}$ DA/0.1 mol $L^{-1}$ PBS/pH 2.58 at Au/PEDOT-$Au_{nano}$...SDS modified electrode at different scan rates (10–150 mV $s^{-1}$), the inset; Linear relationship of $I_p$ vs. $\nu^{1/2}$ for 1 mmol $L^{-1}$ DA at Au/PEDOT-$Au_{nano}$ (●), and Au/PEDOT-$Au_{nano}$...SDS (○) electrodes.

$$I_{pa}(A) = (1.12 \times 10^{-6}) - (5.41 \times 10^{-5})\nu^{1/2} \quad (2)$$

$$I_{pc}(A) = (-1.11 \times 10^{-6}) + (4.95 \times 10^{-5})\nu^{1/2} \quad (3)$$

$$I_{pa}(A) = (1.03 \times 10^{-5}) - (1.37 \times 10^{-4})\nu^{1/2} \quad (4)$$

$$I_{pc}(A) = (-6.29 \times 10^{-6}) + (8.76 \times 10^{-5})\nu^{1/2} \quad (5)$$

The anionic surfactant SDS affects remarkably the diffusion component of the charge transfer at the electrode surface as indicated by the $D_{app}$ values [17].

### 3.4. Effect of solution pH

The effect of changing the pH of the supporting electrolyte on the electrochemical response of DA was studied. Fig. 4 shows the CVs of 1 mmol $L^{-1}$ DA in 0.1 mol $L^{-1}$ PBS of pH 2.58, 4.00,

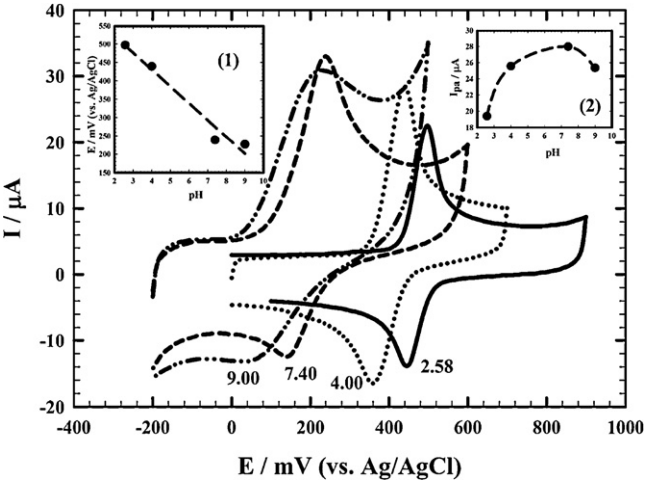


**Fig. 4.** CVs of 1 mmol $L^{-1}$ DA/0.1 mol $L^{-1}$ PBS of different pH: 2.58, 4.00, 7.40, and 9.00 at Au/PEDOT-$Au_{nano}$...SDS modified electrode, inset (1); The dependence of the anodic peak potential of DA on pH value of the solution, and inset (2); the dependence of the anodic peak current of DA on pH value of the solution at Au/PEDOT-$Au_{nano}$...SDS.

Please cite this article in press as: N.F. Atta, et al., Gold nanoparticles-coated poly(3,4-ethylene-dioxythiophene) for the selective determination of sub-nano concentrations of dopamine in presence of sodium dodecyl sulfate, Electrochim. Acta (2012), doi:10.1016/j.electacta.2012.02.082

**Table 1**
Comparison for determination of DA at various modified electrodes based on literature reports.

| Electrode | Compound | pH | LDR (μM) | Sensitivity (μA/μM) | LOD (nM) | Reference |
|---|---|---|---|---|---|---|
| CPE/$Au_{nano}$ | DA | 7.4 | 0.1–6 | 0.288 | 5.9 | [11] |
| GC/CA/$Au_{nano}$ | DA | 7.0 | 0.01–25 | 9.79 | 4 | [5] |
| Pt/PEDOT in presence of SDS | DA | 7.4 | 0.5–25 | NR | 61 | [17] |
| Pt/PMPy/$Pd_{nano}$ | DA | 7.4 | 0.1–10 | 0.71 | 12 | [19] |
| Pt/PMT/$Pd_{nano}$ | DA | 7.4 | 0.05–1 | 1.44 | 8 | [20] |
| GC/$Au_{nano/pedot}$ | DA | 7.4 | 0.5–2 | 850 | 2 | [23] |
| GCE/PEDOT/Pd | DA | 7.4 | 0.5–1 | 1.9 | 500 | [38] |
| Au/PEDOT-$Au_{nano}$...SDS | DA | 7.4 | 0.5–20 | 0.0381 | 0.39 | This work |

*Note*: LDR, linear dynamic range; LOD, limit of detection; NR, not reported; CPE, carbon paste electrode; GC, glassy carbon electrode; CA, cysteamine; Pt, platinum electrode; PMPy, poly(N-methylpyrrole); $Pd_{nano}$, palladium nanoparticles; PMT, poly(3-methylthiophene); $Au_{nano/pedot}$, PEDOT incorporated gold nanoparticles.

7.40, and 9.00 at Au/PEDOT-$Au_{nano}$ electrode in presence of 200 μL of 0.1 mol $L^{-1}$ SDS (the total concentration of SDS after 20 additions is $1.3 \times 10^{-3}$ mol $L^{-1}$). It is clear that changing the pH of the supporting electrolyte altered both the peak potentials and the peak currents of DA. Both the anodic and the cathodic peak potentials shifted negatively with the increase in the solution pH [11,19–22], indicating that the electrocatalytic oxidation of DA at the Au/PEDOT-$Au_{nano}$...SDS is a pH-dependent reaction and protonation/deprotonation is taking part in the charge transfer process. Inset (1) of Fig. 4 shows the relationship between the anodic peak potential and the solution pH value (over the pH range of 2.58–7.40) could be fit to the linear regression equation (Eq. (6)) with a correlation coefficient of $R^2 = 0.994$.

$$E_{pa}(\mathrm{V}) = (0.646) - (0.055)\mathrm{pH} \quad (6)$$

The slope was −0.055 V/pH units over the pH range 2.58–7.40, which is close to the theoretical value of −0.059 V/pH. This indicated that the number of protons and transferred electrons involved in the oxidation mechanism is equal. As the DA oxidation is a two-electron process, the number of protons involved was also predicted to be two indicating a $2e^-/2H^+$ process. In solution, the $pK_a$ values of DA are 8.90 ($pK_{a1}$) and 10.6 ($pK_{a2}$). A little deviation from linearity occurs at pH 9.00, indicating the deprotonation of DA at pH 9.00 so that it is no longer a two-proton, two-electron process at this point and other equilibria should be taken into account [19–22]. Inset (2) of Fig. 4 shows the relationship between the anodic peak current and the solution pH value, the anodic peak current increased from pH 2.58 to pH 7.40 where it reached its maximum value and decreased again at pH 9.00. The highest oxidation peak current was obtained at pH 7.40 (pH medium of the human body).

### 3.5. Determination of DA at physiological pH using Au/PEDOT-$Au_{nano}$ in presence of SDS

The voltammetric behavior of DA was examined using linear sweep voltammetry (LSV) with scan rate 50 mV $s^{-1}$. Inset (1) of Fig. 5 shows typical LSV of standard additions of 0.5 mmol $L^{-1}$ DA/0.1 mol $L^{-1}$ PBS/pH 7.40 to 200 μL of 0.1 mol $L^{-1}$ SDS in 15 mL of 0.1 mol $L^{-1}$ PBS/pH 7.40. Inset (1) of Fig. 5 shows that by increasing the concentration of DA, the anodic peak current increases which indicates that the electrochemical response of DA is apparently improved by SDS due to the enhanced accumulation of protonated DA via electrostatic interaction with negatively charged SDS at the Au/PEDOT-$Au_{nano}$ electrode surface. Fig. 5 and inset (2) show the calibration curves of the anodic peak current values in the linear range of 25–140 μmol $L^{-1}$ DA with the regression equation (Eq. (7)) and 0.5–20 μmol $L^{-1}$ with the regression equation (Eq. (8)) with correlation coefficients of 0.9987, and 0.9978, sensitivities of 0.0387 μA/μmol $L^{-1}$, and 0.0381 μA/μmol $L^{-1}$, detection limits of 1.55 nmol $L^{-1}$ and 0.39 nmol $L^{-1}$, and quantification limits of 5.17 nmol $L^{-1}$, and 1.31 nmol $L^{-1}$, respectively.

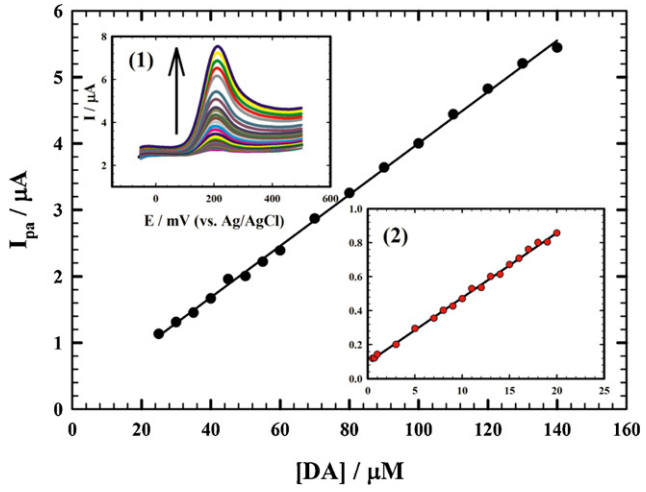


**Fig. 5.** Calibration curve for DA for concentrations from (25 μmol L−1 to 140 μmol $L^{-1}$) and from (0.5 μmol $L^{-1}$ to 20 μmol $L^{-1}$, inset 2), inset 1; LSVs of 15 ml of 0.1 mol $L^{-1}$ PBS/pH 7.40 at Au/PEDOT-$Au_{nano}$...SDS modified electrode in different concentrations of DA (0.5–140 μmol $L^{-1}$), scan rate 50 mV $s^{-1}$.

$$I_p \ (\mathrm{A}) = (1.331 \times 10^{-7}) + 3.871 \times 10^{-8} c \ \ (\mu\mathrm{mol\ L^{-1}}) \quad (7)$$

$$I_p \ (\mathrm{A}) = (9.517 \times 10^{-8}) + 3.814 \times 10^{-8} c \ \ (\mu\mathrm{mol\ L^{-1}}) \quad (8)$$

The detection limit (DL) and quantification limit (QL) were calculated from Eqs. (9) and (10), respectively

$$\mathrm{DL} = 3s/b \quad (9)$$

$$\mathrm{QL} = 10s/b \quad (10)$$

where $s$ is the standard deviation and $b$ is the slope of the calibration curve. Table 1 shows the comparison for the determination of DA at Au/PEDOT-$Au_{nano}$...SDS with various modified electrodes based in literature reports.

### 3.6. Analysis of tertiary mixture at Au/PEDOT-$Au_{nano}$ modified electrode in presence of SDS

The determination of catecholamines in biological samples is crucial for the diagnosis of many diseases. However, electrochemical oxidation of catecholamines especially DA at conventional electrodes is found difficult because of: (i) fouling of the electrode surface due to the adsorption of oxidation products, (ii) interference due to the co-existence of interfering compounds such as ascorbic acid (AA) and others in the biological fluids, and (iii) AA is oxidized at almost the same potential as DA [19–22]. Acetaminophen (paracetamol), APAP, is another drug that likely to interfere with DA and AA determination [21,22,46]. Fig. 6 shows the cyclic voltammogram of tertiary mixture of 1 mmol $L^{-1}$ AA, 1 mmol $L^{-1}$ DA and,

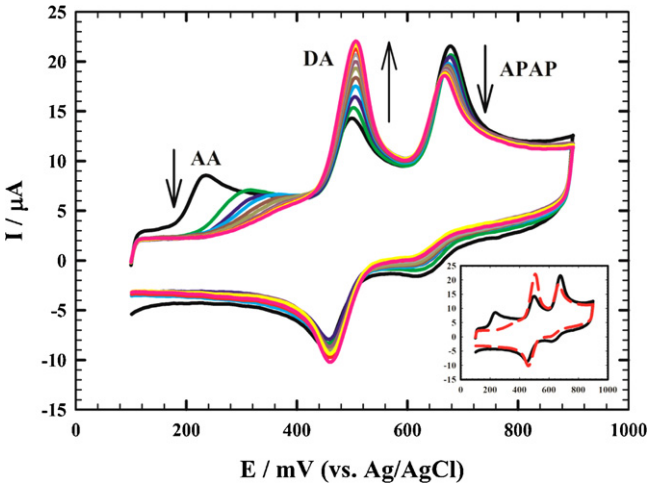


**Fig. 6.** CVs of 1 mmol $L^{-1}$ AA, 1 mmol $L^{-1}$ DA, and 1 mmol $L^{-1}$ APAP in 0.1 mol $L^{-1}$ PBS/pH 2.58 at Au/PEDOT-$Au_{nano}$ with successive additions of (0–200 μL) of 0.1 mol $L^{-1}$ SDS, inset represents the initial (in absence of SDS) and final (in presence of 200 μL SDS) CVs, scan rate 50 mV $s^{-1}$.

1 mmol $L^{-1}$ APAP in 0.1 mol $L^{-1}$ PBS/pH 2.58 at Au/PEDOT-$Au_{nano}$ with successive additions of (0–200) μL of 0.1 mol $L^{-1}$ SDS (increments add $6.7 \times 10^{-5}$ mol $L^{-1}$ SDS of each addition and the total concentration of SDS after 20 additions is $1.3 \times 10^{-3}$ mol $L^{-1}$). The inset of Fig. 6 shows the CVs of the mixture (AA, DA, and APAP) in the absence of SDS and presence of 200 μL of 0.1 mol $L^{-1}$ SDS. Three well-defined oxidation peaks were obtained at Au/PEDOT-$Au_{nano}$ modified electrode at 235, 499, and 678 mV for AA, DA, and APAP, respectively. Thus, Au/PEDOT-$Au_{nano}$ electrode can be used for the simultaneous determination of AA, DA, and APAP in their mixture. By the successive additions of 10 μL of 0.1 mol $L^{-1}$ SDS in the mixture solution, the oxidation peak current of DA increases while the oxidation current of AA decreases till its complete disappearance and the oxidation current of APAP decreases slightly. Surfactants tend to adsorb at different interfaces at concentration below and/or above its critical micellar concentration. Thus, it is expected that the addition of SDS will result in the formation of a surfactant film over the Au/PEDOT-$Au_{nano}$ electrode. This amphiphilic film will align in a way where the head groups of surfactant molecules face the aqueous medium leaving the rest hydrophobic part in contact with each other and away from the aqueous medium. It is clear that there is a negatively charged surface; behind this negative surface there is a hydrophobic region due to the alignment of the surfactant tails. Consequently, the negative charge of the adsorbed surfactant film as well as the hydrophobic character of the interior of this film will act to repel hydrophilic AA molecules or its $AA^-$ away from the electrode surface while enhancing the preconcentration/accumulation of the hydrophobic $DA^+$ cations. The slight decrease in the anodic peak current of APAP may be attributed firstly to its structure in which it behaves neutral in the pH of study, and its diffusion towards the Au/PEDOT-$Au_{nano}$ electrode is slow in comparison with other cationic compounds. Secondly, its interaction with the anionic SDS is retarded as it became neutral compound. The peak current of DA is enhanced at Au/PEDOT-$Au_{nano}$...SDS compared to that of other electrodes, even in the presence of AA and APAP. This clearly shows the synergism between the polymer matrix, gold nanoparticles, and SDS.

### 3.7. Stability of the modified electrode

The stability of Au/PEDOT-$Au_{nano}$...SDS was studied via repeated cycles up to 50 cycles. The inset of Fig. 7(A) shows

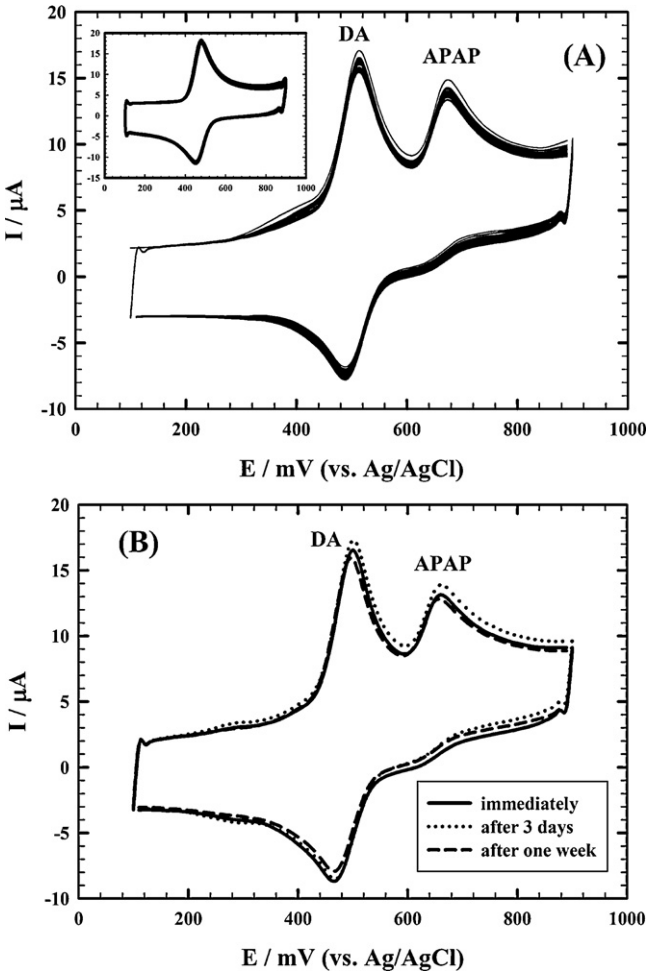


**Fig. 7.** (A) Stability of Au/PEDOT-$Au_{nano}$...SDS for tertiary mixture (1 mmol $L^{-1}$ AA, 1 mmol $L^{-1}$ DA, and 1 mmol $L^{-1}$ APAP/0.1 mol $L^{-1}$ PBS/pH 2.58) separation, 50 repeated cycles, the inset; Stability of Au/PEDOT-$Au_{nano}$...SDS modified electrode in 1 mmol $L^{-1}$ DA/0.1 mol $L^{-1}$ PBS/pH 2.58, 50 repeated cycles, (B) CVs of the comparison of 50th cycle of long term stability of Au/PEDOT-$Au_{nano}$...SDS for tertiary mixture (1 mmol $L^{-1}$ AA, 1 mmol $L^{-1}$ DA, and 1 mmol $L^{-1}$ APAP/0.1 mol $L^{-1}$ PBS/pH 2.58) separation immediately, after 3 days and one week of storage, scan rate 50 mV $s^{-1}$.

the repeated cycles up to 50 cycles of Au/PEDOT-$Au_{nano}$...SDS in 1 mmol $L^{-1}$ DA/0.1 mol $L^{-1}$ PBS/pH 2.58. Excellent stability without any noticeable decrease in the current response was obtained. Thus, both anodic and cathodic peak currents remained relatively stable indicating that this modified electrode has a good reproducibility and does not suffer from surface fouling during the repetitive voltammetric measurement [17]. Also, we noticed that very small peak separation, almost zero or 15 mV peak separation is obtained indicating that unusual high reversibility is obtained by repeated cycles. Fig. 7(A) shows the repeated cycles stability up to 50 cycles for separation of tertiary mixture of 1 mmol $L^{-1}$ AA, 1 mmol $L^{-1}$ DA, and 1 mmol $L^{-1}$ APAP in 0.1 mol $L^{-1}$ PBS/pH 2.58 at Au/PEDOT-$Au_{nano}$...SDS modified electrode. Also, the long term stability for separation of tertiary mixture of AA, DA, and APAP at Au/PEDOT-$Au_{nano}$...SDS modified electrode was studied up to one week. After each measurement, the electrode is stored in 0.1 mol $L^{-1}$ PBS/pH 2.58 in the refrigerator. Fig. 7(B) shows the CVs of the 50th cycle of repeated cycles of Au/PEDOT-$Au_{nano}$...SDS for tertiary mixture of 1 mmol $L^{-1}$ AA, 1 mmol $L^{-1}$ DA, and 1 mmol $L^{-1}$ APAP/0.1 mol $L^{-1}$ PBS/pH 2.58 immediately, after 3 days, and one week. After one week of storage, $I_{pa}$ of DA decreases by 6.7% and $I_{pa}$ of APAP

Please cite this article in press as: N.F. Atta, et al., Gold nanoparticles-coated poly(3,4-ethylene-dioxythiophene) for the selective determination of sub-nano concentrations of dopamine in presence of sodium dodecyl sulfate, Electrochim. Acta (2012), doi:10.1016/j.electacta.2012.02.082

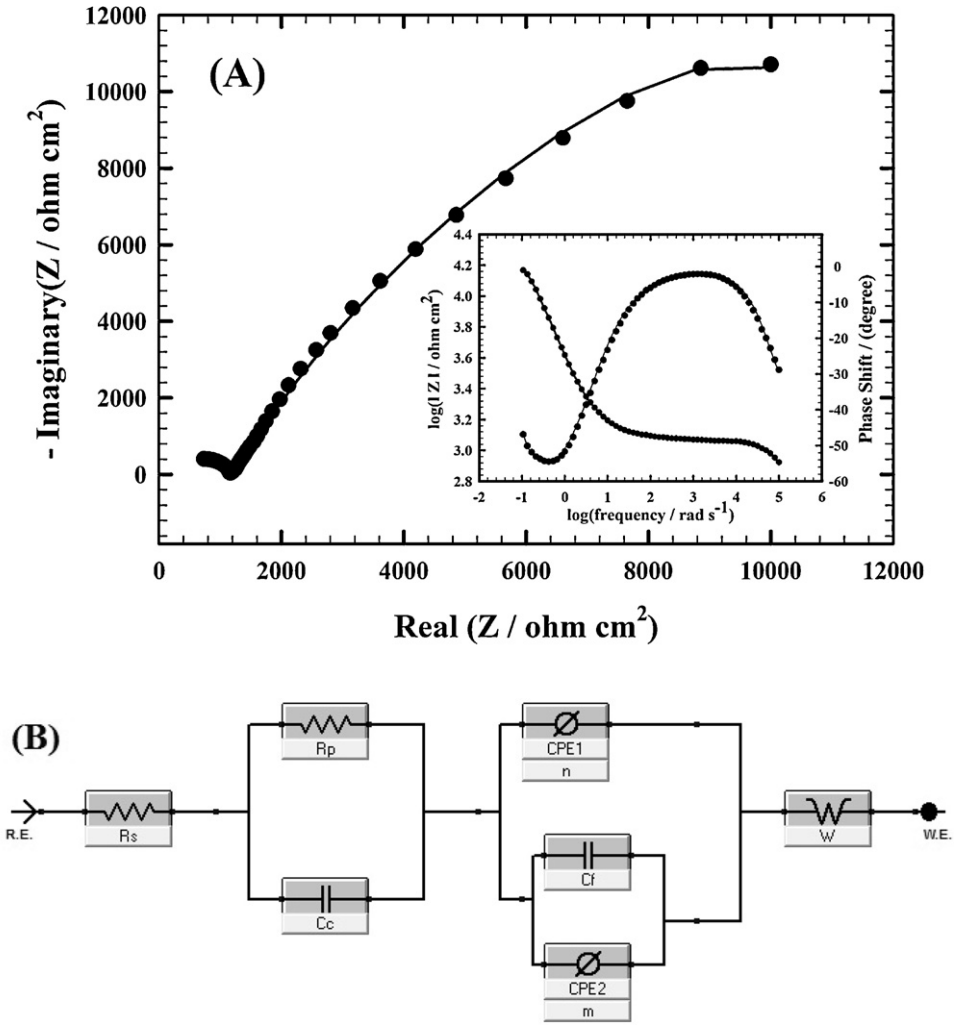


**Fig. 8.** (A) Nyquist plot of Au/PEDOT-$Au_{nano}$. . .SDS modified electrode in 1 mmol $L^{-1}$ DA/0.1 mol $L^{-1}$ PBS/pH 7.40 at the oxidation potential (240 mV), and the inset, the typical impedance spectrum presented in the form of Bode plot. (symbols and solid lines represent the experimental measurements and the computer fitting of impedance spectra, respectively), frequency range: 0.1–100,000 Hz, (B) The equivalent circuit used in the fit procedure of the impedance spectra.

decreases by 1.2%. Thus Au/PEDOT-$Au_{nano}$. . .SDS gives better stability via repeated cycles and long term stability, not only for DA detection (one component), but also, for the separation of tertiary mixture components.

### 3.8. Electrochemical impedance spectroscopy (EIS) of DA

It is well known that the EIS technique is a useful tool for studying the interface properties of surface-modified electrodes [17]. Therefore, EIS was used to investigate the nature of DA interaction at Au/PEDOT-$Au_{nano}$. . .SDS surface. EIS data were obtained for the modified electrode at AC frequency varying between 0.1 Hz and 100 kHz with an applied potential (240 mV) in the region corresponding to the electrolytic oxidation of 1 mmol $L^{-1}$ DA/0.1 mol $L^{-1}$ PBS/pH 7.40. Moreover, the electrochemical system studied is compared with an "equivalent circuit" that uses some of the conventional circuit elements, namely resistance, capacitance, diffusion, and induction elements [11,19–22]. Fig. 8(A) shows a typical impedance spectrum presented in the form of Nyquist plot of DA at Au/PEDOT-$Au_{nano}$. . .SDS modified electrode and the inset shows the typical impedance spectrum presented in the form of Bode plot. The equivalent circuit is shown in Fig. 8(B). In this circuit, $R_s$ is the solution resistance, and $R_p$ is the polarization resistance. Capacitors

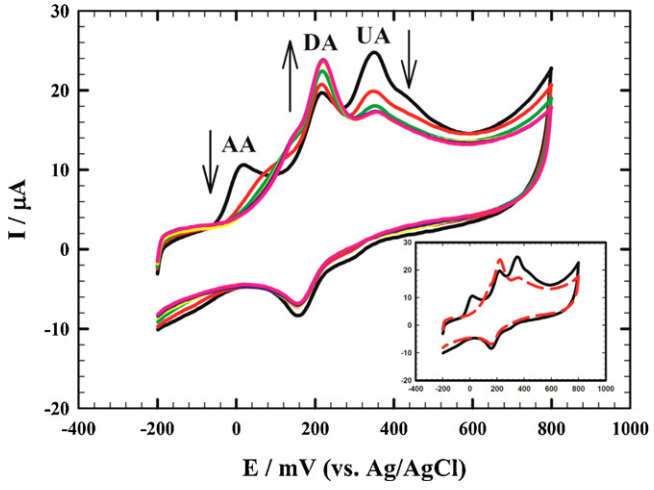


**Fig. 9.** CVs of tertiary mixture of 1 mmol $L^{-1}$ AA, 0.5 mmol $L^{-1}$ DA, and 0.5 mmol $L^{-1}$ UA in 0.1 mol $L^{-1}$ PBS/pH 7.40 at Au/PEDOT-$Au_{nano}$ modified electrode with successive additions of (0–200 µL) of 0.1 mol $L^{-1}$ SDS, inset represents the initial (in absence of SDS) and final (in presence of 200 µL SDS) CVs, scan rate 50 mV $s^{-1}$.

**Table 2**
EIS fitting data corresponding to Fig. 8 (A).

| $R_s/10^2\ \Omega\,cm^2$ | $C_c/10^{-9}$ F cm$^{-2}$ | $R_p/10^2\ \Omega\,cm^2$ | $W/10^3\ \Omega\,s^{-1/2}$ | CPE1/$10^4$ F cm$^{-2}$ | $n$ | $C_f/10^{-5}$ F cm$^{-2}$ | CPE2/$10^3$ F cm$^{-2}$ | $m$ |
|---|---|---|---|---|---|---|---|---|
| 3.497 | 2.282 | 7.887 | 3.433 | 2.053 | 0.4427 | 3.661 | 1.103 | 0.9870 |

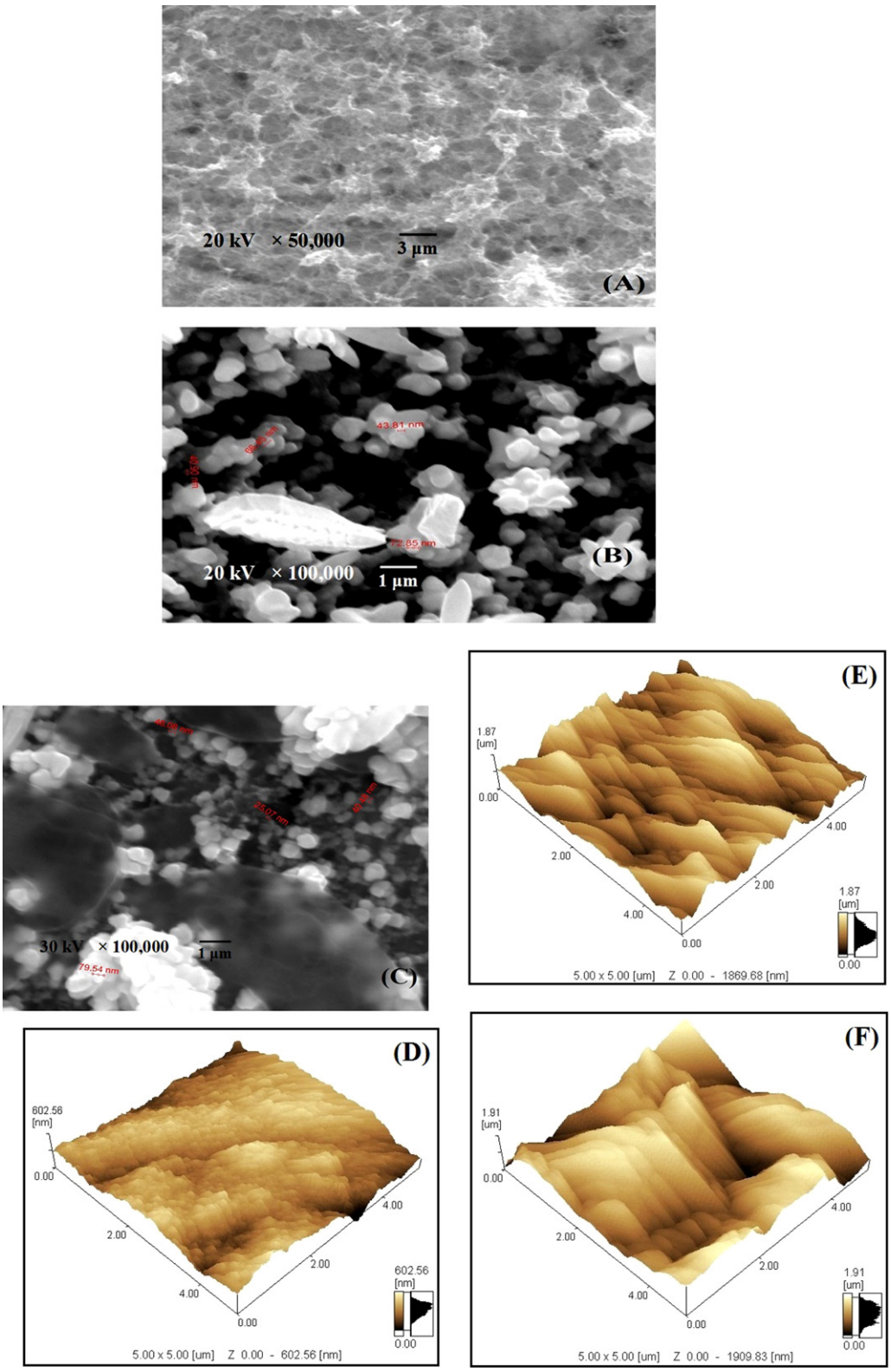


**Fig. 10.** SEM images of: Au/PEDOT (A), Au/PEDOT-Au$_{nano}$ (B), and Au/PEDOT-Au$_{nano}$. . .SDS (C) electrodes, and 3D AFM images of Au/PEDOT (D), Au/PEDOT-Au$_{nano}$ (E), and Au/PEDOT-Au$_{nano}$. . .SDS (F) electrodes by non-contact mode.

Please cite this article in press as: N.F. Atta, et al., Gold nanoparticles-coated poly(3,4-ethylene-dioxythiophene) for the selective determination of sub-nano concentrations of dopamine in presence of sodium dodecyl sulfate, Electrochim. Acta (2012), doi:10.1016/j.electacta.2012.02.082

**Table 3**
Evaluation of the accuracy and precision of the proposed method for the determination of DA in urine sample.

| Sample | Concentration of DA added ($\mu$mol L$^{-1}$) | Concentration of found DA ($\mu$mol L$^{-1}$) | Recovery (%) | Standard deviation $\times 10^{-8}$ | Standard error $\times 10^{-8}$ |
|---|---|---|---|---|---|
| 1 | 1.00 | 1.01 | 101 | 1.64 | 0.822 |
| 2 | 5.00 | 5.07 | 101.4 | 1.81 | 0.904 |
| 3 | 10.0 | 9.94 | 99.4 | 0.687 | 0.343 |
| 4 | 20.0 | 19.7 | 98.5 | 3.03 | 1.52 |
| 5 | 35.0 | 34.9 | 99.7 | 1.73 | 0.867 |

in EIS experiments do not behave ideally; instead they act like a constant phase element (CPE). Therefore, CPE1 and CPE2 are constant phase elements and $n$, and $m$ are their corresponding exponent ($n$ is less than one, and $m$ is nearly one). $C_c$ and $C_f$ represent the capacitance of the double layer [19–22]. Diffusion can create impedance known as the Warburg impedance $W$. Table 2 lists the best fitting values calculated from the equivalent circuit (Fig. 8(B)) for the impedance data of Fig. 8(A). As shown in Fig. 8(A), the impedance spectra include a semicircle portion at the higher frequencies and a linear portion ended with plateau at the lower frequencies, which describe the electron-transfer limiting electrochemical process, and the diffusion-limiting electrochemical process, respectively. The semicircle diameter equals the interfacial charge transfer resistance $R_{ct}$. This resistance controls the electron transfer kinetics of the redox probe at the electrode interface. Therefore, $R_{ct}$ can be used to describe the interface properties of the electrode. The semicircle part in Fig. 8(A) is relatively small, implying a low charge transfer resistance $R_{ct}$ of the redox probe which is attributed to the selective interaction between SDS and DA that resulted in the observed current signal increase for the electrooxidation process and this indicates the conductivity and the high catalytic activity of the modified electrode and the facilitation of charge transfer. The values of the capacitive component indicating the conducting character of the modified surface due to ionic adsorption at the electrode surface and the charge transfer process.

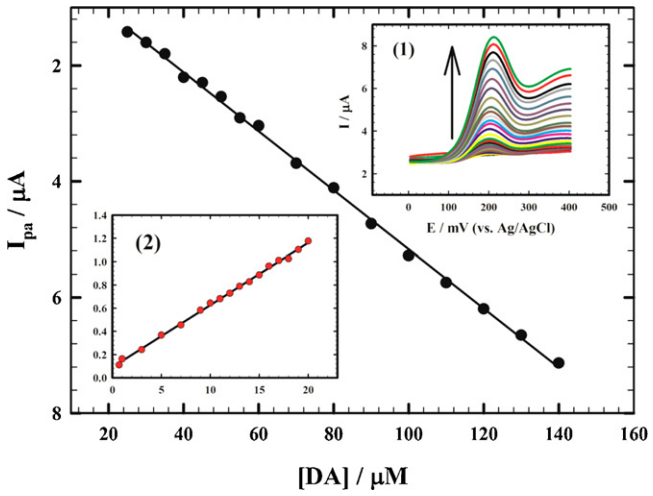


**Fig. 11.** Calibration curve for DA for concentrations from (25 $\mu$mol L$^{-1}$ to 140 $\mu$mol L$^{-1}$) and from (0.7 $\mu$mol L$^{-1}$ to 20 $\mu$mol L$^{-1}$, inset 2), (stock solution of DA was prepared in urine), inset (1); LSVs of 15 ml of 0.1 mol L$^{-1}$ PBS/pH 7.40 at Au/PEDOT-Au$_{nano}$. . .SDS in different concentrations of DA (0.7–140 $\mu$mol L$^{-1}$), scan rate 50 mV s$^{-1}$.

### 3.9. Electrochemistry of DA in presence of UA and AA

DA, UA and AA coexist in the extracellular fluid of the central nervous system and serum [11,17,19,35,36]. The ability to selectively determine these species has been a major goal of electroanalysis research. Therefore, the electrochemical behaviors of DA, UA and AA in a mixture solution were studied. Fig. 9 shows the CVs of 0.5 mmol L$^{-1}$ DA in tertiary mixture with 1 mmol L$^{-1}$ AA and 0.5 mmol L$^{-1}$ UA at Au/PEDOT-Au$_{nano}$ with the successive additions of (0–200) $\mu$L of 0.1 mol L$^{-1}$ SDS in the mixture solution (0.1 mol L$^{-1}$ PBS, pH 7.40). The inset of Fig. 9 shows the CVs of the mixture (DA, UA, and AA) in absence of SDS and presence of 200 $\mu$L SDS. The oxidation peaks are resolved at Au/PEDOT-Au$_{nano}$ electrode with the peak potentials at 349 mV, 217 mV, and 19 mV for UA, DA, and AA, respectively. The large separation of the peak potentials allows selective and simultaneous determination of UA, DA, or AA in their mixture. The oxidation peak current for DA increased from 10.7 $\mu$A in absence of SDS to 20 $\mu$A in presence of SDS. Moreover, the oxidation peak current for both AA and UA are suppressed. The high response for DA was observed due to the electrostatic interaction of the anionic surfactant with the protonated DA ($pK_a = 8.92$) in pH 7.40, but in case of AA and UA repulsion takes place as AA ($pK_a = 4.10$) and UA ($pK_a = 5.4$) are in the anionic form and in micellar medium they established an electrostatic repulsion with anionic surfactant SDS, which provokes a large decrease in the peak current value. This indicates that the accumulation of SDS on the modified electrode forms a negative layer on the electrode surface. Therefore, we can determine DA selectively in the presence of AA, and UA. The change of the peak current values for AA, UA and DA after adding SDS can be assigned to the spontaneous adsorption of the surfactant onto electrode surface, which may change the overpotential of the electrode and influence the electron transfer rate. Also, the formation of micellar aggregates may influence the mass transport of electroactive species to the electrode [17].

### 3.10. Surface morphologies of the different modified electrodes

The response of an electrochemical sensor was related to the physical morphology of its surface. Fig. 10(A)–(C) shows the SEM images of Au/PEDOT, Au/PEDOT-Au$_{nano}$ and Au/PEDOT-Au$_{nano}$. . .SDS electrodes, respectively and from SEM images, a significant difference in morphology was observed for PEDOT, PEDOT-Au$_{nano}$, and Au/PEDOT-Au$_{nano}$. . .SDS. The morphology of PEDOT film (Fig. 10(A)) has globular morphology and the surface looks rough due to the Au substrate. The SEM image of PEDOT-Au$_{nano}$ (Fig. 10(B)) shows that metallic nanoparticles are located at different elevations over the PEDOT film exhibiting a large surface area. In presence of SDS (Fig. 10(C)), PEDOT-Au$_{nano}$ film becomes spongy due to the presence of anionic tailing structure. Thus, the aggregates of SDS that accumulates onto the surface of PEDOT-Au$_{nano}$ shown in the SEM picture influences the conductivity level of the film and helps the attraction of DA (selectively) to the surface of the electrode. Atomic force microscopy is a powerful tool to measure topography and properties of surfaces. Typical AFM 3D images of Au/PEDOT, Au/PEDOT-Au$_{nano}$, and Au/PEDOT-Au$_{nano}$. . .SDS electrodes by the non-contact mode are shown in. Fig. 10(D)–(F), respectively.

Please cite this article in press as: N.F. Atta, et al., Gold nanoparticles-coated poly(3,4-ethylene-dioxythiophene) for the selective determination of sub-nano concentrations of dopamine in presence of sodium dodecyl sulfate, Electrochim. Acta (2012), doi:10.1016/j.electacta.2012.02.082

### 3.11. Determination of DA in human urine samples

The utilization of the proposed method in real sample analysis was also investigated by direct analysis of DA in human urine. The same measurements were conducted successfully on urine samples. In this set of experiments, DA was dissolved in urine to make a stock solution with 0.5 mmol $L^{-1}$ concentration. Inset (1) of Fig. 11 shows typical LSV of standard additions of 0.5 mmol $L^{-1}$ DA in urine to 200 μL of 0.1 mol $L^{-1}$ SDS in 15 mL of 0.1 mol $L^{-1}$ PBS/pH 7.40 at Au/PEDOT-$Au_{nano}$. The calibration curves of DA in urine in the linear range of 25–140 μmol $L^{-1}$, and 0.7–20 μmol $L^{-1}$ are shown in Fig. 11 and inset (2), respectively. The detection limits of 1.77 nmol $L^{-1}$, and 0.56 nmol $L^{-1}$ with correlation coefficients of 0.9987, and 0.9983 are obtained, respectively. Five different concentrations on the calibration curve are chosen to be repeated to evaluate the accuracy and precision of the proposed method, which is represented in Table 3. The recovery ranged from 98.5% to 101.4%, and the results are acceptable indicating that the present procedures are free from interferences of the urine sample matrix. The results strongly proved that DA can be selectively and sensitively determined at Au/PEDOT-$Au_{nano}$...SDS modified electrode in urine sample.

## 4. Conclusions

In this work, a novel approach of synergism between the conducting polymer matrix, gold nanoparticles, and SDS is explored for DA sensing in the presence of UA, and excess AA in 0.1 mol $L^{-1}$ PBS/pH 7.40. The PEDOT matrix is recognized to be responsible for the peak separation (selectivity) while also favouring catalytic oxidation of the above compounds. Gold nanoparticles with SDS allow sub-nanomolar sensing of DA (sensitivity). The utilization of anionic surfactants in electroanalytical applications is described in this work. The negatively charged SDS adsorbed onto the electrode surface control the electrode reactions of AA, UA and DA that differ in their net charge. SDS forms a monolayer on Au/PEDOT-$Au_{nano}$ surface with a high density of negatively charged end directed outside the electrode which enhances the accumulation of protonated DA via electrostatic interactions and improves DA oxidation current signal while the corresponding signals for AA and UA are quenched via electrostatic repulsion. We also demonstrated the selective and simultaneous determination of tertiary mixture of AA, DA, and APAP using Au/PEDOT-$Au_{nano}$...SDS modified electrode. Au/PEDOT-$Au_{nano}$...SDS modified electrode gives better stability via repeated cycles and long term stability. Very small peak separation, almost zero or 15 mV peak separation is obtained indicating that unusual high reversibility is obtained by repeated cycles. The present modified electrode showed high reproducibility, selectivity, sensitivity, relatively lower detection limit, and better stability, not only for DA detection (one component), but also, for the separation of tertiary mixture components.

## Acknowledgments

The authors would like to acknowledge the financial support from Cairo University through the Vice President Office for Research Funds.

## References

[1] J. Li, H. Xie, L. Chen, Sens. Actuators B 153 (2011) 239.
[2] M. Chen, G. Diao, Talanta 80 (2009) 815.
[3] Y. Hu, Y. Song, Y. Wang, J. Di, Thin Solid Films 519 (2011) 6605.
[4] R.N. Goyal, V.K. Gupta, M. Oyama, N. Bachheti, Talanta 72 (2007) 976.
[5] G.-Z. Hu, D.-P. Zhang, W.-L. Wu, Z.-S. Yang, Colloids Surf. B 62 (2008) 199.
[6] R.N. Goyal, A. Aliumar, M. Oyama, J. Electroanal. Chem. 631 (2009) 58.
[7] J. Li, X. Lin, Sens. Actuators B 124 (2007) 486.
[8] D. Feng, F. Wang, Z. Chen, Sens. Actuators B 138 (2009) 539.
[9] J. Wang, W.-D. Zhang, J. Electroanal. Chem. 654 (2011) 79.
[10] Y. Song, Y. Ma, Y. Wang, J. Di, Y. Tu, Electrochim. Acta 55 (2010) 4909.
[11] N.F. Atta, A. Galal, F.M. Abu-Attia, S.M. Azab, J. Electrochem. Soc. 157 (9) (2010) F116.
[12] H. Guan, P. Zhou, X. Zhou, Z. He, Talanta 77 (2008) 319.
[13] A.R. Goncalves, M.E. Ghica, C.M.A. Brett, Electrochim. Acta 56 (2011) 3685.
[14] F.S. Belaidi, P.T. Boyer, P. Gros, J. Electroanal. Chem. 647 (2010) 159.
[15] C.-Y. Lin, V.S. Vasantha, K.-C. Ho, Sens. Actuators B 140 (2009) 51.
[16] F.S. Belaidi, D. Evrard, P. Gros, Electrochem. Commun. 13 (2011) 423.
[17] N.F. Atta, A. Galal, R.A. Ahmed, Bioelectrochemistry 80 (2011) 132.
[18] A. Kros, N.A.J.M. Sommerdijk, R.J.M. Nolte, Sens. Actuators B 106 (2005) 289.
[19] N.F. Atta, M.F. El-Kady, A. Galal, Anal. Biochem. 400 (2010) 78.
[20] N.F. Atta, M.F. El-Kady, Sens. Actuators B 145 (2010) 299.
[21] N.F. Atta, M.F. El-Kady, Talanta 79 (2009) 639.
[22] N.F. Atta, M.F. El-Kady, A. Galal, Sens. Actuators B 141 (2009) 566.
[23] J. Mathiyarasu, S. Senthilkumar, K.L.N. Phani, V. Yegnaraman, Mater. Lett. 62 (2008) 571.
[24] S.V. Selvaganesh, J. Mathiyarasu, K.L.N. Phani, V. Yegnaraman, Nanoscale Res. Lett. 2 (2007) 546.
[25] M.A.G. Namboothiry, T. Zimmerman, F.M. Coldren, J. Liu, K. Kim, D.L. Carroll, Synth. Met. 157 (2007) 580.
[26] B.Y. Kim, M.S. Cho, Y.S. Kim, Y. Son, Y. Lee, Synth. Met. 153 (2005) 149.
[27] S. Harish, J. Mathiyarasu, K.L.N. Phani, Mater. Res. Bull. 44 (2009) 1828.
[28] C. Zanardi, F. Terzi, R. Seeber, Sens. Actuators B 148 (2010) 277.
[29] C. Zanardi, F. Terzi, L. Pigani, A. Heras, A. Colina, J.L. Palacios, R. Seeber, Electrochim. Acta 53 (2008) 3916.
[30] S.S. Kumar, J. Mathiyarasu, K.L. Phani, J. Electroanal. Chem. 578 (2005) 95.
[31] F. Terzi, C. Zanardi, V. Martina, L. Pigani, R. Seeber, J. Electroanal. Chem. 619 (2008) 75.
[32] K.M. Manesh, P. Santhosh, A. Gopalan, K.P. Lee, Talanta 75 (2008) 1307.
[33] Y.-P. Hsiao, W.-Y. Su, J.-R. Cheng, S.-H. Cheng, Electrochim. Acta 56 (2011) 6887.
[34] S. Thiagarajan, S.-M. Chen, Talanta 74 (2007) 212.
[35] X. Lin, Y. Zhang, W. Chen, P. Wu, Sens. Actuators B 122 (2006) 309.
[36] A. Safavi, N. Maleki, O. Moradlou, F. Tajabadi, Anal. Biochem. 359 (2006) 224.
[37] S. Lupu, C. Lete, M. Marin, N. Totir, P.C. Balaure, Electrochim. Acta 54 (2009) 1932.
[38] S. Harish, J. Mathiyarasu, K.L.N. Phani, V. Yegnaraman, J. Appl. Electrochem. 38 (2008) 1583.
[39] Y. Chen, L.-R. Guo, W. Chen, X.-J. Yang, B. Jin, L.-M. Zheng, X.-H. Xia, Bioelectrochemistry 75 (2009) 26.
[40] R.K. Shervedani, M. Bagherzadeh, S.A. Mozaffari, Sens. Actuators B 115 (2006) 614.
[41] C. Li, Y. Ya, G. Zhan, Colloids Surf. B 76 (2010) 340.
[42] N.F. Atta, S.A. Darwish, S.E. Khalil, A. Galal, Talanta 72 (2007) 1438.
[43] N.F. Atta, A. Galal, F.M.A. Attia, S.M. Azab, Electrochim. Acta 56 (2011) 2510.
[44] G.A. Angeles, S.C. Avendaño, M.P. Pardavé, A.R. Hernández, M.R. Romo, M.T.R. Silva, Electrochim. Acta 53 (2008) 3013.
[45] J. Zheng, X. Zhou, Bioelectrochemistry 70 (2008) 408.
[46] S.-F. Wang, F. Xie, R.-F. Hu, Sens. Actuators B 123 (2007) 495.

Please cite this article in press as: N.F. Atta, et al., Gold nanoparticles-coated poly(3,4-ethylene-dioxythiophene) for the selective determination of sub-nano concentrations of dopamine in presence of sodium dodecyl sulfate, Electrochim. Acta (2012), doi:10.1016/j.electacta.2012.02.082